

A Single Layer 3-D Touch Sensing System for Mobile Devices Application

Li Du, *Student Member, IEEE*, Chun-Chen Liu, *Senior Member, IEEE*, Yan Zhang, Yilei Li, Yuan Du, *Student Member, IEEE*, Yen-Cheng Kuan, *Member, IEEE*, and Mau-Chung Frank Chang, *Fellow, IEEE*

Abstract—Touch sensing has been widely implemented as a main methodology to bridge human and machine interactions. The traditional touch sensing range is 2-D and therefore limits the user experience. To overcome these limitations, we propose a novel 3-D contactless touch sensing called Airtouch system, which improves user experience by remotely detecting single/multi-finger position. A single layer touch panel with triangle-shaped electrodes is proposed to achieve multitouch detection capability as well as manufacturing cost reduction. Moreover, an oscillator-based-capacitive touch sensing circuit is implemented as the sensing hardware with the bootstrapping technique to eliminate the interchannel coupling effects. To further improve the system accuracy, a grouping algorithm is proposed to group the useful channels' data and filter out hardware noise impact. Finally, improved algorithms are proposed to eliminate the fringing capacitance effect and achieve accurate finger position estimation. EM simulation proved that the proposed algorithm reduced the maximum systematic error by 11 dB in the horizontal position detection. The proposed system consumes 2.3 mW and is fully compatible with existing mobile device environments. A prototype is built to demonstrate that the system can successfully detect finger movement in a vertical direction up to 6 cm and achieve a horizontal resolution up to 0.6 cm at 1 cm finger-height. As a new interface for human and machine interactions, this system offers great potential in finger movement detection and gesture recognition for small-sized electronics and advanced human interactive games for mobile device.

Index Terms—3-D, bootstrapping, correlated double sampling (CDS), finger position, gesture recognition, human machine interaction, interchannel coupling, mobile device, touchscreen.

Manuscript received March 20, 2016; revised July 1, 2016 and November 10, 2016; accepted April 26, 2017. Date of publication May 9, 2017; date of current version January 19, 2018. This paper was recommended by Associate Editor Y. P. Liu. (*Corresponding author: Li Du.*)

L. Du, C.-C. Liu, and Y. Du are with the Department of Electrical Engineering, University of California at Los Angeles, Los Angeles, CA 90095 USA, and also with Kneron Inc., San Diego, CA 92122 USA (e-mail: dl1989113@ucla.edu).

Y. Zhang and M.-C. F. Chang are with the Department of Electrical Engineering, University of California at Los Angeles, Los Angeles, CA 90095 USA.

Y. Li is with the Department of Electrical Engineering, University of California at Los Angeles, Los Angeles, CA 90095 USA, and also with Novumind Inc., Santa Clara, CA 95054 USA.

Y.-C. Kuan is with the Department of Electrical Engineering, University of California at Los Angeles, Los Angeles, CA 90095 USA, and also with National Chiao Tung University, Hsinchu 30010, Taiwan.

Color versions of one or more of the figures in this paper are available online at <http://ieeexplore.ieee.org>.

Digital Object Identifier 10.1109/TCAD.2017.2702630

I. INTRODUCTION

TOUCH sensing, as a major modern human/machine interface (HMI) has been widely implemented in various display products (e.g., smartwatches, mobile phones, tablets, and TV). Modern touch sensing systems, which are low power and light weight, created a user-friendly interface for users to control and manipulate electronic devices. According to a recent market report, there will be 2.8 billion touchscreen shipped to the market in 2016 [1]. In the current touchscreen sensing system market, there are various sensing methodologies, including resistive touch sensing, capacitive touch sensing, and ultrasonic-based sensing [2]. Among them, the capacitive touch sensing is one of the most promising ones due to its high finger position detection resolution, multitouch detection availability, and compatibility with existing display panels [3].

The general capacitive touchscreen is designed with electrodes deposited on top of the display. When a finger touches the screen, it changes the capacitance of the shielded electrodes below. The hardware circuit detects this capacitance change and reconstructs the finger position. However, this technology requires physical contacts and hence creates several disadvantages, such as unresponsiveness with wet hands, a limited resolution with shrinking screen size and unavoidable fingerprint residues on the screen surface. In addition to that, the advanced mobile entertainment systems require an improved HMI to capture human's motion in front of the screen which traditional 2-D touch sensing cannot support.

To overcome aforementioned challenges, 3-D touch sensing technology has been proposed recently and implemented in many large-display electronic devices. The 3-D touch sensing technology, referred to as contactless sensing, aims to detect user instructions by detecting finger position at certain height and also recognizing hand gestures or finger movements. Hu *et al.* [4] reported the capability of sensing gestures' motion up to 30 cm in height in front of a display with customized electrodes. Reference [5] achieves up to 10 cm motion track by depositing two large layer electrodes on the touch panel. Among these reported works, employing large electrodes on a display is a common approach. It plays a critical role in mitigating the electrodes' coupling effects and increasing the sensed finger capacitance. However, this approach not only requires a large-sized touch panel but also consumes large power consumption due to the size of the electrodes, making

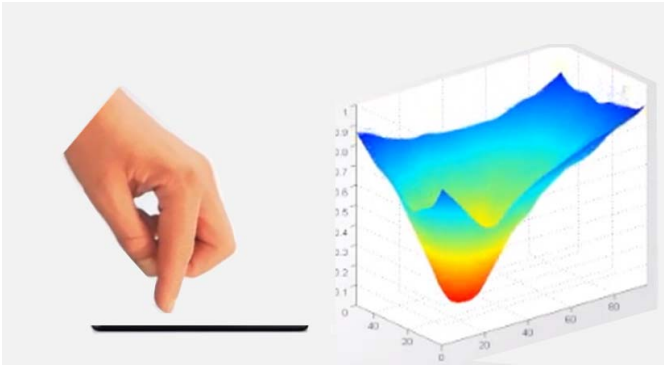


Fig. 1. Concept of Airtouch sensing showing noncontact interface using capacitive sensing to detect finger position.

it unusable for mobile devices, where screen size and power is limited and electrode fabrication cost is expensive.

To implement 3-D touch sensing technology into volume and power-constrained mobile devices with low cost, a new single-layer 3-D touch sensing system called Airtouch has been invented. This system is designed to accommodate the space and power constraints of the mobile device environment. It is designed to enable the system to detect the human finger position and gestures remotely when fingers are approaching the screen, as shown in Fig. 1. The system consists of a low-cost single-layer mobile touchscreen, a highly sensitive capacitive sensing circuit as in [6], and a corresponding finger 3-D position detection algorithm that can be programmed into the mobile device's application processor. Specially, we make the following contributions.

- 1) We propose a new single layer touch panel pattern design for 3-D touch sensing that solves the traditional ghost point problems in the self-capacitive multitouch sensing and reduces the touchscreen manufacturing cost by half compared with regular two-layer touchscreen.
- 2) We invent a bootstrapped-oscillator-based correlated double sampling (BCDS) capacitive sensing hardware circuit that can eliminate electrode coupling effects and enable accurate finger capacitance detection.
- 3) We propose an improved grouping filter as compared to [7] for 3-D touch sensing back-ground noise reduction and potential multitouch position detection.
- 4) We improve the algorithms by considering the finger's fringing capacitance effect in the position detection.
- 5) We demonstrate the potential 3-D single/multi-touch detection in our mobile-sized prototype systems.

The remainder of this paper is organized as follows. Section II describes the comparison of different capacitive touch sensing methodology and the proposed single layer touch panel design with its corresponding electrical model. Section III explains the proposed hardware sensing circuit and its innovations in solving the existing touch sensing problems. Section IV describes the corresponding software algorithms built up in this prototype and the relevant verified EM simulation. Section V reports the performance of this 3-D touch sensing system in real-world scenarios. Finally, Section VI concludes this paper.

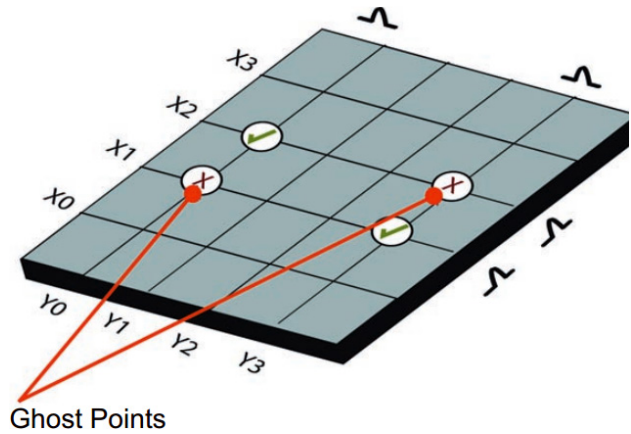


Fig. 2. Touch screen is touched with two fingers that are diagonally separated and detected through self-capacitive sensing, a pair of “ghost points” are created because the controller only knows that two columns and two rows have been touched; it cannot tell which coordinate pairs belong.

II. TOUCH PANEL DESIGN AND MODELING

This section first compares the difference between two capacitive sensing methodologies and then we propose the single layer self-capacitive touch panel design for 3-D touch sensing and its corresponding electrical model.

A. Sensing Methodology Comparison

The current 2-D capacitive touch sensing can be mainly categorized as the self-capacitive sensing and mutual-capacitive sensing [8]. For self-capacitive sensing, the sensor senses the finger induced self-capacitance change to the shielded electrodes; for mutual capacitive sensing, the change is shown on the coupling capacitance between horizontal and vertical electrodes. Although the parasitic mutual capacitance of the touch electrode is generally much larger than the self-capacitance, mutual capacitive sensing is still widely used as the main 2-D touch sensing methodology in the mobile industry due to its compatibility of implementing multitouch detection. For self-capacitive sensing, multitouch detection cannot be supported due to the potential generation of ghost point during electrode scanning [9] as shown in Fig. 2.

Compared to 2-D touch sensing, the contactless nature of 3-D touch sensing has created an air gap between the finger and the thin touch glass. This requires the touch panel's electrodes to sense a much smaller finger capacitance [10]. Fig. 3 shows a comparison of the induced capacitance with the finger in different height. As illustrated, when the finger is not touching the screen, the induced capacitance value is reduced by $10\times$ time. This large active capacitance reduction results in a reduction of the system sensitivity which makes the normal mutual capacitive sensing inapplicable for mobile 3-D sensing. For Airtouch, we have implemented self-capacitive sensing as our system sensing methodology to achieve maximum system sensitivity.

B. Single Layer 3-D Touch Panel Design

As described above, one of the drawbacks for the common two-layer touch panel is that it is unable to detect multifinger

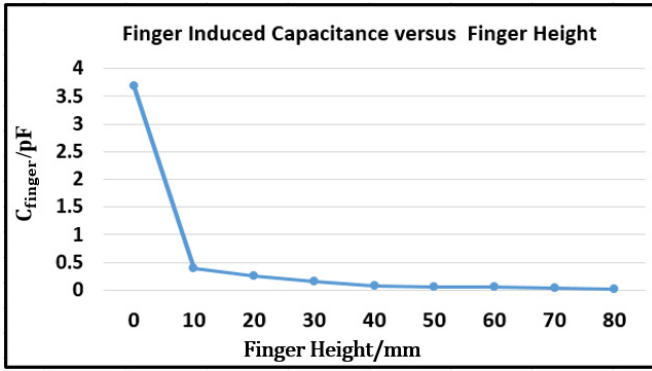


Fig. 3. Finger-induced capacitance on the electrode versus finger height. The finger has been represented as a 10 cm height grounded-cylinders with a radius of 0.5 cm [11].

position through self-capacitive sensing. In addition, the design cost of a two-layer touch panel is much higher than the single-layer touch panel.

To overcome these two issues, we have proposed a single-layer touch panel pattern design that can support multitouch detection through self-capacitance sensing and aimed at reducing the fabrication cost by half through using only one-layer electrodes. The sensing electrodes have been designed as triangular shapes as opposed to the normal diamond shapes. This provides a Y direction detection ability through calculating the upper channels' and lower channels' detected finger-capacitance ratio.

Moreover, this structure also avoids the generation of diagonal ghost points which limits the traditional self-capacitive touch sensing in multitouch detection. The triangular-shaped electrodes may create an ambiguity regarding of the multifingers' position if the fingers are exactly aligned in the same X direction, however, this is a recoverable position error as opposed to the totally different diagonal ghost points that occurs in the standard two-layer touch panel. Fig. 4 gives an example of this type of the touch panel with six channels. However, the real number of the channels can be changed depending on the applications and hardware availability.

C. Touch Panel Modeling

In addition to the touch panel pattern design, the suitable electrical modeling of the touch panel also plays an important role in defining hardware circuit specifications and evaluating the system performance. The electrodes of the touch panel are usually fabricated through depositing indium tin oxide (ITO) on the screen with a sheet resistance between 10 and 100 ohm/square [12]. This large sheet resistance provides a routing resistance that cannot be ignored in the touch panel modeling. Also, each touch electrode will have a self-capacitance to the ground and mutual capacitance to its nearby electrodes. The self-to-ground capacitance serves as an additional load for the detection circuit, reducing the system sensitivity. In addition, the mutual capacitance creates a shorting path from electrodes to electrodes, limiting the accuracy of the finger position estimation.

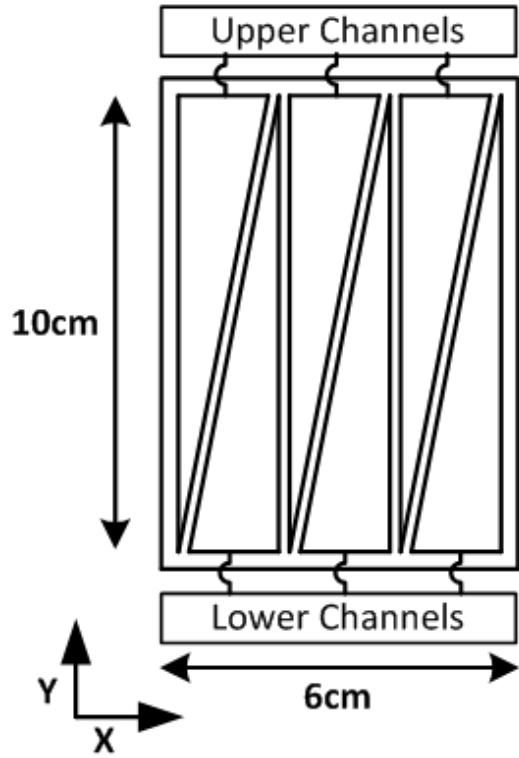


Fig. 4. Example of the triangular single-layer touch panel design.

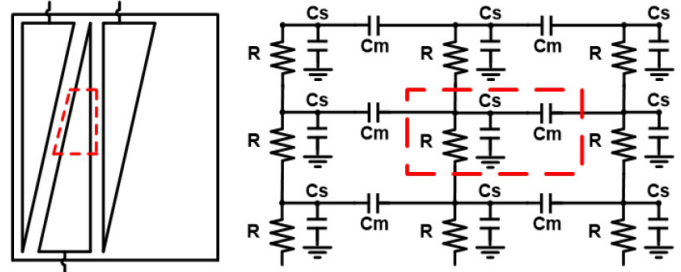


Fig. 5. Modeling of the touch electrode with one unit portion highlighted.

In order to accurately model each parameter's effect on the system performance, the long electrode is deposited into several portions, providing an RC constant of each portion that is much smaller than the sensing signal's periods. Fig. 5 shows an example of depositing the electrode into three discrete lumped RC units. In each unit, C_s represents the electrode's self-capacitance of that particular portion, while C_m represents the coupling capacitance to its nearby parallel electrode. The C_s and C_m can be obtained through an EM simulation while the R can be calculated based on the analytical expression

$$R = R_s \times \frac{2L}{3}(W_u + W_d) \quad (1)$$

where the R_s is the sheet resistance of the ITO, L is the length of the electrode on Y direction, and W_u , W_d correspond to the upper and lower width of the electrode's on X direction's in each portion. In the following section, we will describe the hardware self-capacitive sensing circuit implemented in the Airtouch system.

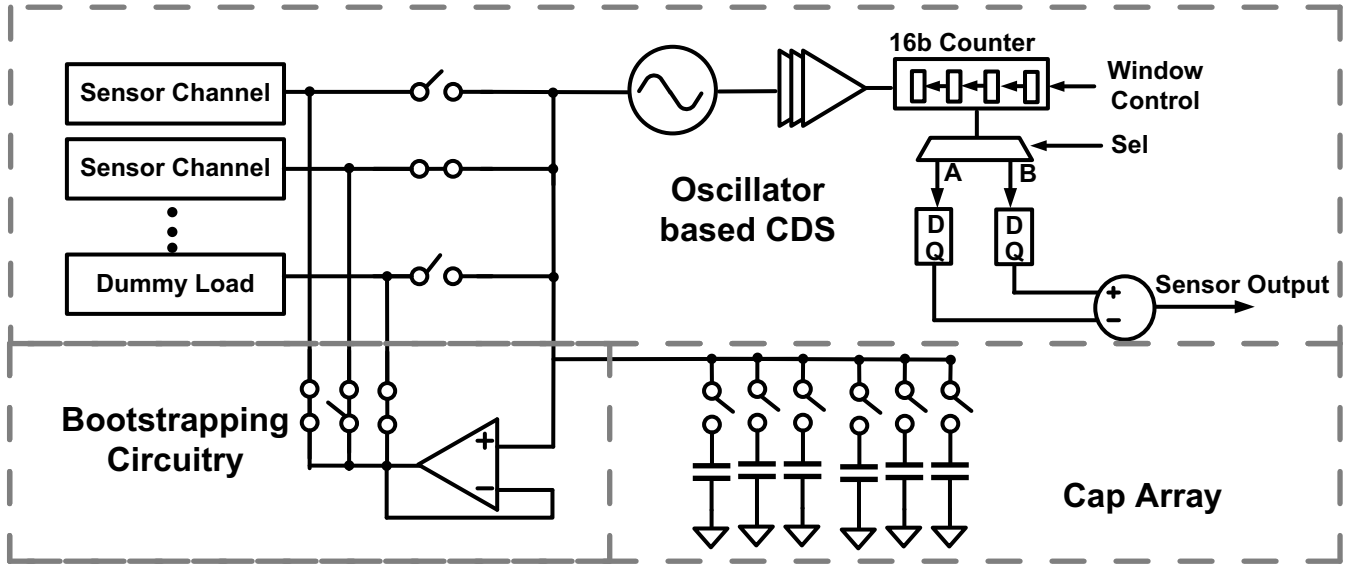


Fig. 6. Airtouch system hardware circuit.

III. AIRTOUCH HARDWARE CIRCUITRY DESIGN

In this section, we provide the hardware sensing circuit design for the whole Airtouch system, including correlated double sampling (CDS) technique used to improve system sensitivity and bootstrapping circuitry to reduce interchannel coupling effects of the touch panel.

A. Hardware System Architecture

An overall hardware diagram of the Airtouch system is shown in Fig. 6. The hardware circuit is implemented as described in [6]. The system contains an oscillator-based CDS module with trimming capacitor array at the oscillator input to enable high resolution self-capacitive sensing and a bootstrapping circuitry to reduce the interchannel coupling effects.

The major sensing blocks of the BCDS system is an inverter-based LC oscillator with its load capacitor end connected to the touch electrode. The channel's load capacitance change is measured by monitoring the frequency change of the oscillator. This is achieved through a digital counter integrating the number of pulses coming from the oscillator in a fixed time window. To remove the common noise effect and improve system sensitivity, a CDS method has been implemented through using a dummy load to cancel the channel's intrinsic self-capacitance. In each acquisition, the oscillator is first connected to the desired input sensor channel for a given integration time and then connected to a dummy load with similar capacitance for the same integration time. By comparing the counter's output code difference, the finger capacitance value can be derived as

$$C_{\text{finger}} = \Delta C = \frac{1}{4\pi^2(f - \Delta f)^2 L} - \frac{1}{4\pi^2 f^2 L} \approx \frac{\Delta f}{2\pi^2 f^3 L}. \quad (2)$$

The benefits of the CDS is that if the dummy channel's and active channel's load properties are well-matched, the system can cancel most of the low frequency noise (i.e., flick noise, thermal induced frequency drift) by generating a zero at the

dc in its frequency response. The equivalent transfer function of the CDS can be derived as

$$\begin{aligned} Y(t) &= \int_{t-t_0}^t X(t) - \int_t^{t+t_0} X(t) \\ &= \int_{-\infty}^t 2X(t) - X(t-t_0) - X(t+t_0) \end{aligned} \quad (3)$$

$$\begin{aligned} H(f) &= \frac{F(Y(t))}{F(X(t))} = \frac{1}{j2\pi f} (2 - e^{j2\pi t_0 f} - e^{-j2\pi t_0 f}) \\ &= \frac{4\sin(\pi t_0 f)^2}{j2\pi f} = -2j \sin c(\pi t_0 f) t_0 \sin(\pi t_0 f) \end{aligned} \quad (4)$$

where t_0 is the integration window time. When f is close to dc, the transfer function can be approximated as (5), showing a zero at the dc

$$H(f) = -2\pi j \sin c(\pi t_0 f) t_0^2 f. \quad (5)$$

B. Bootstrapping Technique to Reduce Interchannel Coupling

Although the sensing mechanism is self-capacitive sensing, the large interchannel coupling capacitance can also limit the system sensitivity, causing a resolution degradation in the horizontal direction during the channel scanning process. For example, when the finger is hovering over one channel, the small fringing capacitance is directly coupled to the other channels through the interchannel coupling capacitance which gives an unwanted response in the other channels. Reference [13] has mitigated this problem through grounding all unused channels, however, this results a dramatically increase of the parasitic capacitance which degrade the system sensitivity.

To avoid sensitivity degradation and meanwhile isolate the interchannel coupling, a bootstrapped circuitry has been implemented as Fig. 7. The coupling capacitance is nullified through a tracking amplifier which senses the time-domain voltage of the currently active channel and replicate it on the remaining

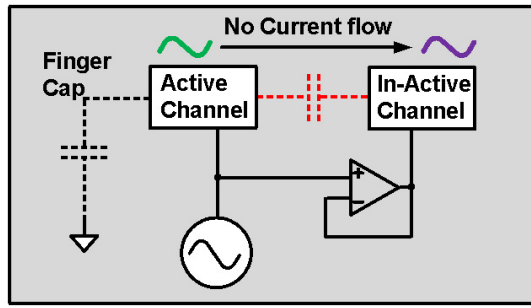


Fig. 7. Introduced bootstrapped circuitry showing the suppression of the coupling capacitance through the tracking amplifier.

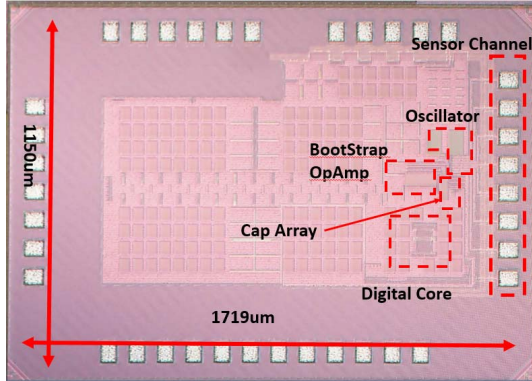


Fig. 8. Airtouch hardware circuit die photograph.

inactive channels. By embedding this tracking amplifier, the coupling capacitance viewed from the input has been reduced to $1/A$ of its original value [14].

The proposed Airtouch hardware sensing circuit's die photograph is shown in Fig. 8 with labeled dimensions and components. In the following sections, we will introduce the algorithm that used to estimate the finger's position through the readout capacitance value in each channels.

IV. FINGER POSITION AND ALGORITHM

In this section, we describe the improved algorithms used in finger position detection. The whole backend digital processing procedures are shown in Fig. 9. The acquired channel's self-capacitance values first go to a group filter to remove noise effect and then the processed data will be used to calculate finger's instant X , Y , Z direction position separately. Finally, the instant position information goes to the reconstruction blocks to estimate the current finger position.

A. Grouping Filter

As described in Section III, the potential unwanted coupling capacitance of the touch panel can cause system performance degradation, resulting in inaccurate finger positioning. Even the bootstrapping technique described before has mostly canceled the coupling capacitance; a small fractional leaked capacitance can still create finger position error. In addition, the body-introduced background capacitance is also sensed during the scanning which creates ambiguity for the system to determine real finger position. To avoid this, a grouping filter

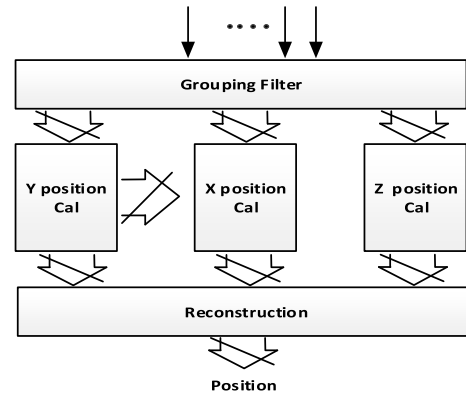


Fig. 9. Airtouch signal processing procedure.

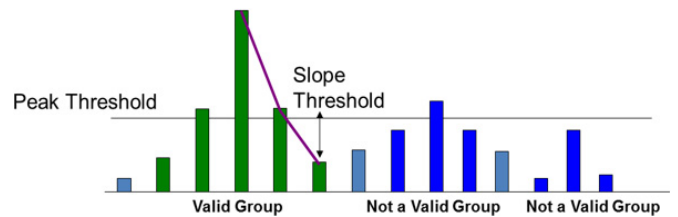


Fig. 10. Illustration of the grouping algorithm to filter out unwanted capacitive response.

is proposed. The grouping filter first categorizes the channel responses into several groups and then applies criterion to all the groups and filters out the groups that do not meet the criterion.

A group of the channel responses can be regarded as a peak envelope in the channel responses (center channel response is more than its left and right response). To further remove the noise effects, a low-level threshold is applied to filter out weak channel response shown as Fig. 10.

After categorizing, the channel responses will be separated into several group responses. Each group will go through the group filter to select the valid groups and filter out the invalid ones. The group filter is configured with two criterions.

- 1) A valid group should have an average slope more than the defined slope threshold.
- 2) In each valid group, at least one channel's response is more than the channel peak threshold.

The peak and slope threshold values are determined through experimenting in the prototype system. The noise of the system can be referred as the standard deviation of the system output without fingers close to it and it is calculated by using raw data from the experiment.

The peak threshold is set to be three times of this standard deviation to remove noise effect. In addition, the noise will also create ambiguity regarding of the finger X direction position when the channel response is weak. Slope threshold is set to be same as the system output standard deviation to reduce this effect.

After the grouping filter, the output data will be passed to each block separately to calculate the instant position in different directions.

B. Y Position Estimation

The horizontal direction instant position estimation is separated into X , Y directions, the system first uses the grouped data to determine the instant Y position and then estimate the instant X position information through the obtained instant Y position information.

The instant Y position information can be obtained through comparing upper and lower channels' response difference. For a certain finger Y positions, the responses of these two different types of channels are different. For example, when a finger is close to the touch panel's upper edge, upper channels will have a much larger response compared to the lower channels due to its large sensing area compared with its nearby lower channel's. By assuming the finger induced capacitance value is proportional to its shielded area, we can derive the Y position as

$$Y_{\text{finger}} = \frac{\sum \Delta C_{\text{upper}} - \sum \Delta C_{\text{lower}}}{\sum \Delta C_{\text{upper}} + \sum \Delta C_{\text{lower}}} Y_{\text{max}}. \quad (6)$$

Here, ΔC_{upper} and ΔC_{lower} represent each measured upper and lower channel's sensed capacitance.

However, this derived equations only fits when the finger capacitance can be modeled as a linear parallel plates' capacitance. As the application aims to detect the finger position with a certain finger height, the induced fringing capacitance need to be accounted for. Fig. 11 shows how this fringing capacitance can affect the detection accuracy. Here, the center vertical arrows represent the linear finger-capacitance modeled as parallel plates' capacitance. In additional, the side surface of the finger also induced certain capacitance in the electrodes' input, causing a position error if using (6) to estimate.

Since fringing capacitance is induced by finger's side surface, we have assumed the upper channels' sensed fringing capacitance is equal to the lower channels sensed fringing capacitance. Based on this assumption, we can derive (6)'s error as (8). This added fringing capacitance generates a large position error when the finger is close to the panel's edge

$$\begin{aligned} Y_{\text{finger}_m} &= \frac{\sum \Delta C_{\text{upper}_m} - \sum \Delta C_{\text{lower}_m}}{\sum \Delta C_{\text{upper}_m} + \sum \Delta C_{\text{lower}_m}} Y_{\text{max}} \\ &= \frac{\sum \Delta C_{\text{upper}_l} - \sum \Delta C_{\text{lower}_l}}{\sum \Delta C_{\text{upper}_l} + \sum \Delta C_{\text{lower}_l} + \sum C_{\text{fringing}}} Y_{\text{max}} \\ Y_{\text{error}} &= \frac{\sum \Delta C_{\text{upper}_l} - \sum \Delta C_{\text{lower}_l}}{\sum \Delta C_{\text{upper}_l} + \sum \Delta C_{\text{lower}_l}} Y_{\text{max}} - Y_{\text{finger}_m} \\ &= \frac{(\sum \Delta C_{\text{upper}_l} - \sum \Delta C_{\text{lower}_l}) C_{\text{fringing}} Y_{\text{max}}}{(\sum \Delta C_{\text{lower}_l} + \sum \Delta C_{\text{upper}_l})(\sum \Delta C_{\text{lower}_l} + \sum \Delta C_{\text{upper}_l} + \sum C_{\text{fringing}})}. \end{aligned} \quad (7)$$

Here, $\Delta C_{\text{upper}_m}$ and $\Delta C_{\text{lower}_m}$ represent the measured upper and lower channels' sensed capacitance. $\Delta C_{\text{upper}_l}$ and $\Delta C_{\text{lower}_l}$ represent the sensed linear finger capacitances of the upper and lower channels. C_{fringing} represents the sensed fringing capacitance in each channel.

To compensate this fringing capacitance effect in the position estimation, we add a fixed coefficient in (6). The final equation is derived as (9) and (10). To further verify the effectiveness of this coefficient on improving the detection resolution, an EM model of the finger and the touch panel is built with the Ansoft Q3D CAD tool as shown in Fig. 11. Simulated

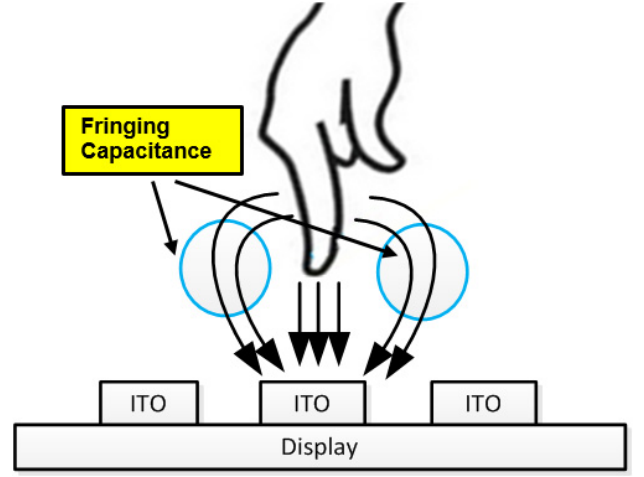


Fig. 11. Illustration of the fringing capacitance effect on the measuring accuracy.

finger-induced capacitance values are put in (6) and (9) to calculate the finger Y position and compare with the real position value in the EM modeling. As shown in Fig. 12, this added coefficient has reduced the maximum position modeling error by 11 dB compared to the reported work in [7]

$$Y_{\text{finger}} = \beta_0 \frac{\sum \Delta C_{\text{upper}_m} - \sum \Delta C_{\text{lower}_m}}{\sum \Delta C_{\text{upper}_m} + \sum \Delta C_{\text{lower}_m}} Y_{\text{max}} \quad (9)$$

$$\beta_0 = \frac{\Delta C_{\text{upper}_l} + \Delta C_{\text{lower}_l} + C_{\text{fringing}}}{\Delta C_{\text{lower}_l} + \Delta C_{\text{upper}_l}}. \quad (10)$$

C. Instant X Position Calculation

The instant X position is calculated based on the center-weighted algorithm. Notice the electrode has different widths in different Y position; how to accurately represent the electrode's center position in X direction plays an important role in determining the actual finger instant position. Here, we use the obtained Y position information to define each electrode's X direction's center position and calculated the finger position based on the weighted average of all the electrodes' center X positions. The algorithm can be separated into the following two steps with the equation shown on (11) and (12).

- 1) Find each electrode's center X_{position} based on the finger's Y position obtained above.
- 2) Calculate the weighted average of all the channels' center X_{position} with their finger capacitive responses and output the average as the final X position

$$X_{\text{center}_i} = \frac{X_{\text{top}_i} + X_{\text{bot}_i}}{2} + \frac{X_{\text{top}_i} - X_{\text{bot}_i}}{2} \times \frac{Y_{\text{finger}}}{Y_{\text{max}}} \quad (11)$$

$$X_{\text{finger}} = \frac{\sum_i X_{\text{center}_i} \times \Delta C_i}{\sum_i \Delta C_i}. \quad (12)$$

Here, X_{center_i} is the i channel's center X_{position} at the certain Y finger value and the X_{top_i} corresponds to the i channel's top-edge's middle point X position; X_{bot_i} represents the i channel's bottom-edge's middle point X position and ΔC_i is the sensed i channel's finger capacitance. These parameters are explained in Fig. 13.

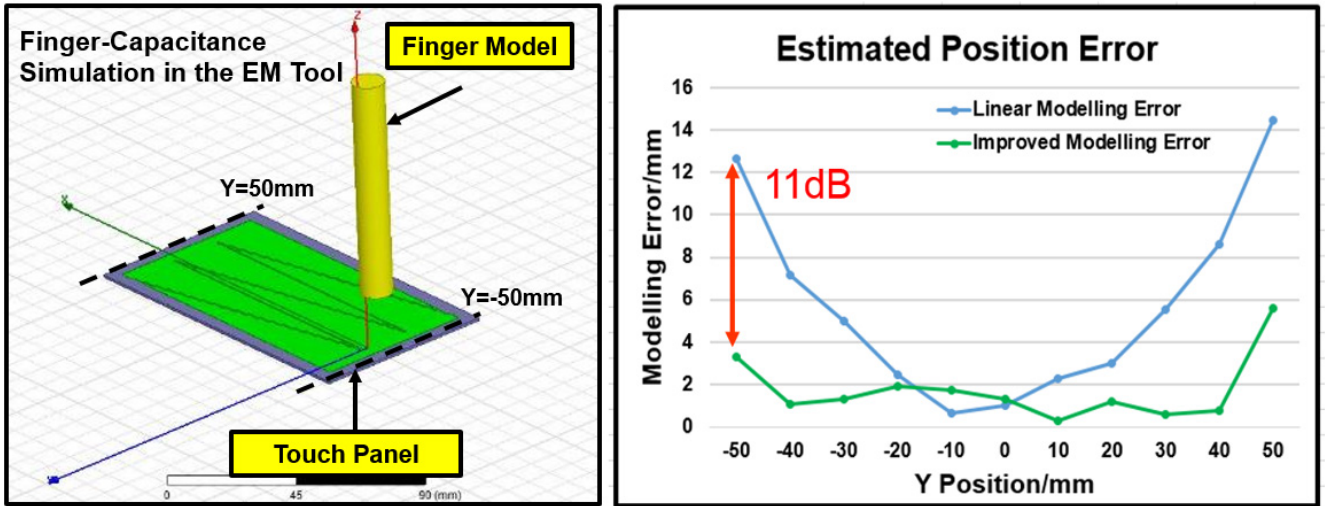


Fig. 12. Illustration of Y position calculation modeling and the comparison of the new proposed equations estimation error versus the old one. Modeling results shows the estimation error is reduced by 11 dB.

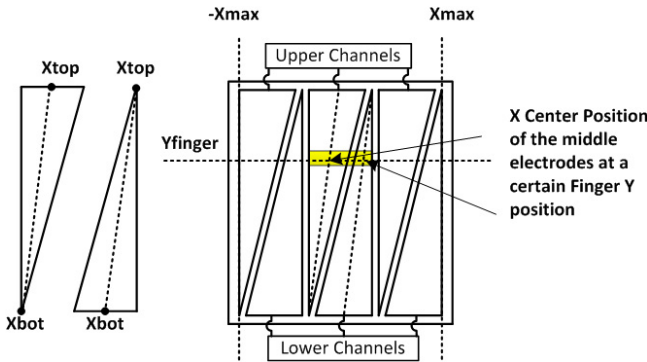


Fig. 13. Electrode's center position calculation at a certain finger Y position.

D. Instant Z Position Calculation

The instant Z position calculation is based on the total measured finger-induced coupling capacitance on the touch panel. As the size of the touch panel is much larger than the user's finger, the finger is modeled as a small circular disk on top of the plane. In this case, the coupling capacitance is a combination of the parallel coupling capacitance and fringing capacitance. Here, the parallel coupling capacitance is inversely proportional to the finger height, while the fringing capacitance has a nonlinear transfer function at a large finger height [15].

To obtain an accurate relationship between the capacitance and finger distance, we have used the polynomial curve to fit the EM simulation results on the finger height versus channel's sensed finger capacitance. Since the application is targeted to be embedded in mobile phones, where computational resources are limited, we have removed the third and above orders to reduce the computation complexity. The Z direction equation can be written as

$$Z_{\text{finger}} = a + \beta_0 \frac{\varepsilon_0 A}{\sum_i \Delta C_i} + \beta_1 \left(\frac{\varepsilon_0 A}{\sum_i \Delta C_i} \right)^2 \quad (13)$$

where a , β_0 , and β_1 are constant coefficients obtained through curve fitting on the EM modeling result, while A represents the finger surface area and ΔC_i corresponds to the i channel's sensed finger capacitance.

To verify the effectiveness of this equation to estimate finger's Z position, we have put our modeled finger and touch panel in the EM tools and simulate the electrode's capacitance response with the finger in different horizontal positions (left, center, and right) and different heights. The obtained capacitance derives the estimated Z position through (13) and is compared with the real finger position in the EM tool shown in Fig. 14. Results shows the estimated error is less than 4 mm for up to 6 cm finger-height.

E. Position Reconstruction

The final reconstructed finger position is based on the instant finger position information obtained from above. Since the finger does not touch the screen, any environmental or systemic noise can result in a large variation on the calculated finger position, making the output finger position unstable. In addition, the environment can also generate some random peak noise due to electromagnetic interference or background change, causing a large finger position jump from sample to sample.

To avoid this, a fifth order IIR filter has been implemented on the reconstruction block to remove random peak noise effect as well as to stabilize the reconstructed finger position. Through using this IIR filter, high frequency noise is removed and output position change is much smoother.

V. EXPERIMENT AND DISCUSSION

In this section, a prototype of the proposed Airtouch 3-D touch sensing system has been built and measured. The first experiment is to check the CDS method in improving the system sensitivity. Then, a comparison of the channel response to different finger position is listed to prove the reduction of the interchannel coupling effect through bootstrapping technique.

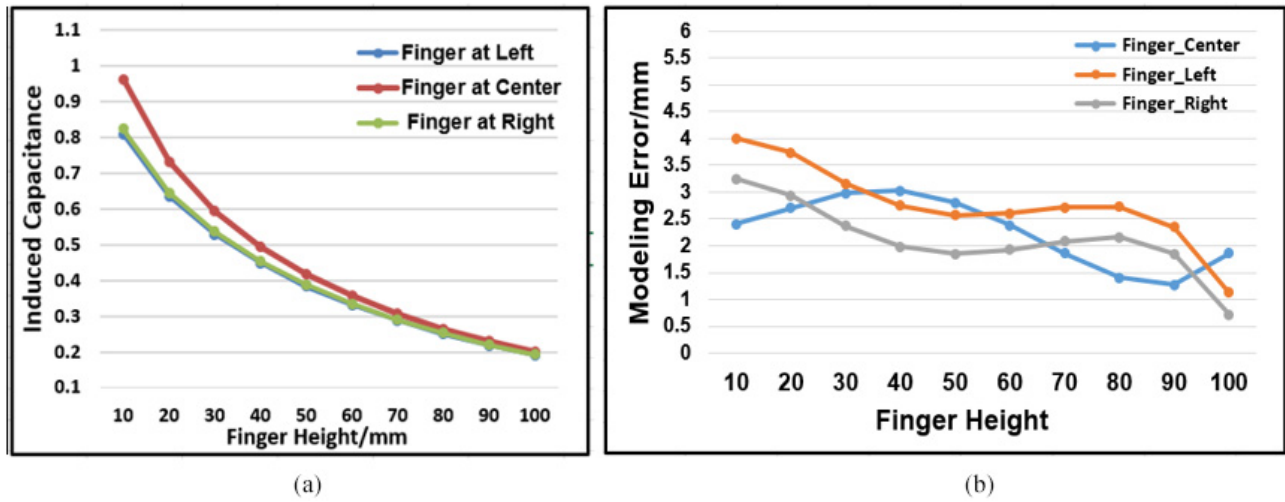


Fig. 14. (a) Finger position versus the sensed capacitance in the EM tools. (b) Estimated position error in Z directions through (13).

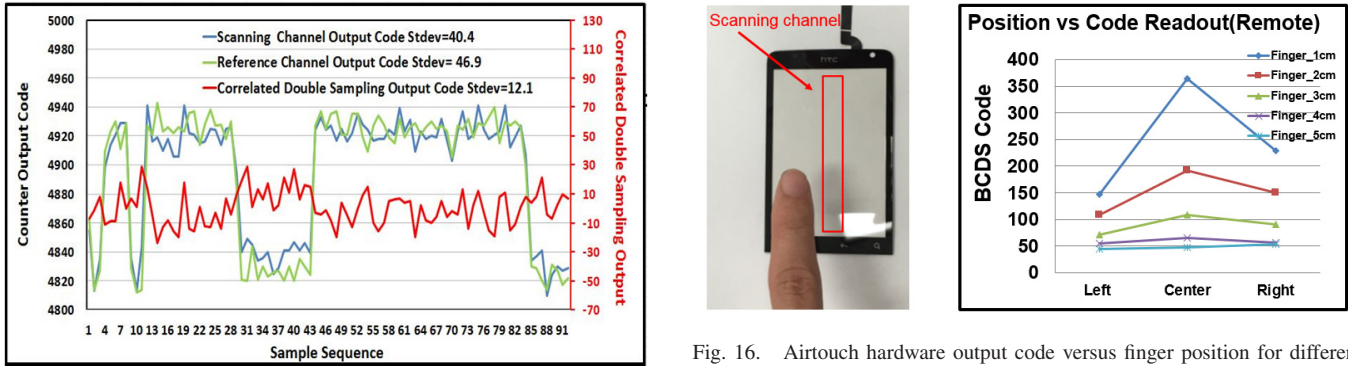


Fig. 15. Measurement of the counter output for the reference channel and an actively channel showing that the oscillator is correlated between both conditions.

Fig. 16. Airtouch hardware output code versus finger position for different finger heights.

Finally, a new Airtouch 3-D sensing system platform has been built and characterized with instant video demonstrations of the system’s concept.

A. Hardware Circuit Measurement

As described in Section II, one of the techniques we implement to improve the hardware sensing resolution is by applying CDS method to reduce the noise in the system. To verify the effectiveness of this method, we connected the prototyped sensor with a standard HTC 3.4” mobile touch screen array (Channel Number: $X = 16$ $Y = 10$) [16].

During the measurement, we first record the sensor’s counter’ output when the sensor is connected to the reference channel (dummy load) and then repeat the measurement with the sensor connected to the active channel. Next, we plot these two cases’ values and compute each case’s standard deviation. Then, we perform the subtraction operation to produce the CDS output. Fig. 15 shows the counter output code for the regular channels as well as the CDS output. Based on the curve of the active channel’s output and reference channel’s output, we see a high levels of correlation between the two. By

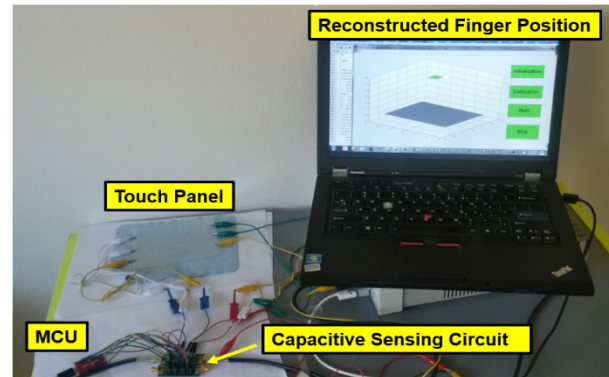


Fig. 17. Airtouch demonstration setup.

comparing the standard deviation of the regular channel output and the CDS output, we see 10.5 dB reduction of system noise through CDS function.

Besides the CDS, the bootstrapping circuitry is another technique we propose to reduce the interchannel coupling effect to improve the hardware circuit resolution for finger position estimation in X, Y direction. To verify this, the sensed channel is fixed to a vertical channel located in the center of the screen as highlighted in Fig. 15. The finger is moving from the left side of the screen to the right side with different heights. The

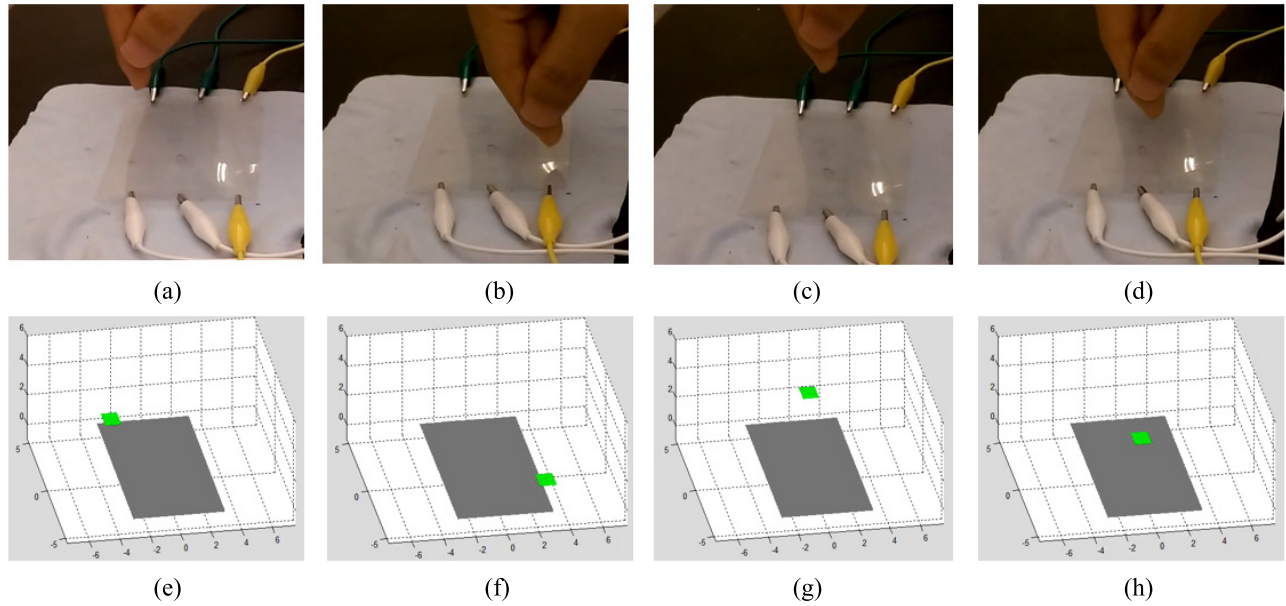


Fig. 18. Comparison of Airtouch sensing result versus real finger position. (a), (b), (c), and (f) Finger horizontal moving comparison. (c), (d), (g), and (h) Finger vertical moving comparison.

TABLE I
PERFORMANCE SUMMARY AND COMPARISON

	ISSCC14 [4]	MGC3130 [5]	This Work
Sensing Type	3D Large Screen	3D Large Screen	3D Mobile
Touch Layer No.	2	2	1
External Component Required	Yes(33uH inductor)	No	No
Screen Size	30cm x 40cm	14.8cm x 9.9cm	10cm x 6cm
Horizontal Resolution	0.7cm	NA	<0.6cm@1cm Finger Height
Z direction detection range	30cm	10cm	6cm
Power Consumption	19mW	66mW	2.3mW
Die Area	4.2mm ²	NA	2mm ²
Supply Voltage	1.2/2.5V	3.3V	1V(sensing circuit) 3.3V(MCU)

measured channel response is shown in Fig. 16. As it shows, when the finger's height is below 3 cm, the bootstrapping circuitry provides sufficient coupling isolation. When the finger is above 3 cm, because of the limited gain of the amplifier and the reduction of the finger-induced capacitance, the bootstrapping circuitry can no longer support the X direction position differentiation.

B. Algorithm Performance Evaluation

The evaluation of the system's algorithm accuracy in finger-position estimation is conducted a prototype setup as Fig. 17. The prototype system contains a mobile-phone-sized touchscreen with a triangular electrode pattern as described before, a low power capacitive sensing circuit to sense the finger capacitance, an ARM-based microprocessor unit (MCU) and a laptop to calculate and display the reconstructed finger position.

The reconstructed finger position is represented as a 1 cm² green square in the coordinate system, while the touch panel is modeled as a gray rectangle with same size as the real panel. The system is real-time updated with a sampling speed up to

30 times per second and a power consumption of 2.3 mW for the hardware sensing circuit. The experiment is conducted with user's finger hovering on top of the screen and moving both horizontally and vertically. Fig. 18 compares the real finger position in space with its reconstructed value in the system.

The experiment shows that the system achieves an X, Y direction resolution up to 0.6 cm (measured at a finger height at 1 cm) through the improved algorithm to reduce the fringing capacitance effect. The horizontal direction resolution reduced when finger height is higher and achieves no differentiation if finger height is more than 4 cm. Experiment shows this resolution reduction is mainly coming from two factors.

- 1) Weak finger-induced capacitance causes the channel-coupling effect dominated and results no channel response difference for different finger positions.
- 2) As the finger height increased the finger fringing capacitance becomes dominated and makes the proposed position estimation model inaccurate.

In addition, the system achieves a Z direction detection range up to 6 cm with a resolution of 1.5 cm. The detection error in Z direction is more than the modeling predictions at a large Z distance. Through experiment, we believe this

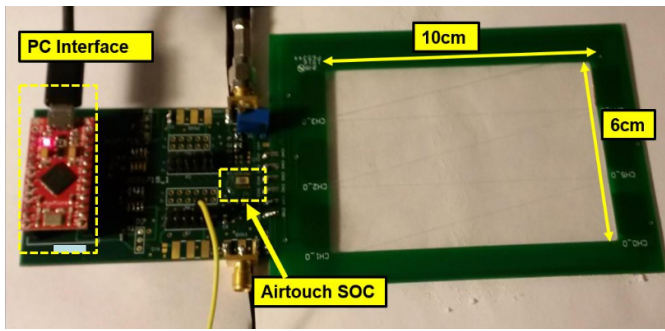


Fig. 19. Airtouch mobile-prototype platform setup.

is mainly caused by simplifying the surrounded environment (i.e., hand shape and body shape) in the EM modeling.

Table I lists the performance summary of the Airtouch system and comparison with other relevant work. Compared to other relevant work, the Airtouch system shows to be more suitable for mobile device, where the power and space are limited

C. Airtouch System Demonstration

To further validate our concept of implementing this technology into mobile devices to provide advanced user-experiences, we built a mobile-prototype platform with our Airtouch system integrated as shown in Fig. 19. Here, the screen is fabricated through depositing ITO on top of plastic PET film.

The first synchronous demo video for single-finger position capture is shown in [17]. The demonstration begins with characterizing the finger horizontal position detection accuracy at a certain finger height (2–3 cm). Next, we perform some simple gestures by drawing circles on top of the screen. Finally, to verify the Z direction detection range, the finger is moved up and down on the screen. As shown in the demonstration video, the prototype platform can capture the user's finger movement on top of the screen successfully through the Airtouch sensing system.

The second synchronous demo video characterizes the system performance to multifinger position detection as shown in [18]. As shown in the video, the system can successfully detect the two-finger's movement in both X, Y, Z direction separately without generating any diagonal ghost point.

D. Discussion

As demonstrated, the Airtouch system offers the potential to improve traditional 2-D mobile touch sensing to 3-D sensing. The demonstrated system focuses on detecting the 3-D finger position and user's gestures with existing mobile hardware device. While this prototype employs a customized hardware sensing circuit, it can be replaced by any existing high resolution capacitive sensor (e.g., [19]).

VI. CONCLUSION

In this paper, we propose and successfully set up a single-layer 3-D touch sensing system to enable remotely

single/multi-finger position detection for mobile devices. The proposed touch panel is implemented in single layer to achieve low production cost and avoid the generation of diagonal ghost point through the proposed electrode's pattern. Moreover, the low power capacitive sensing hardware circuit enable its compatibility with existing mobile device environment. Finally, we invent the corresponding algorithms that are used to filter out background noise, estimate the finger's space position and identify gestures. Our experiment shows that with the improved algorithm to eliminate the fringing capacitances effect, the Airtouch system can achieve a 0.6 cm horizontal resolution at 1 cm finger height and a 6 cm vertical detection range.

The proposed Airtouch system is not limited to mobile device applications though it has been validated as a mobile device HMI interface. Other applications such as Smart TV [20], tablets can also benefit by implementing this technology to improve their user experience. Moreover, emerging wearable devices can also benefit from this technology by implementing the gesture recognition on their small displays. For example, instead of clicking the tiny button on the Apple watch, one can give a rising hand gesture on top of the screen to control the watch.

ACKNOWLEDGMENT

The authors would like to thank TSMC for foundry support and Wintek Corporation for providing a mobile phone touch-screen sample.

REFERENCES

- [1] I. Statista. *Global Shipment Forecast for Touch-Screen Displays From 2012 to 2016*. Accessed on Sep. 1, 2016. [Online]. Available: <http://www.statista.com/statistics/259983/global-shipment-forecast-for-touch-screen-displays>
- [2] L. Du, "Oscillator-based touch sensor with adaptive resolution," M.S. thesis, Dept. Elect. Eng., Univ. California, Los Angeles, CA, USA, 2013.
- [3] M. R. Bhalla and A. V. Bhalla, "Comparative study of various touch-screen technologies," *Int. J. Comput. Appl.*, vol. 6, no. 8, p. 12, Sep. 2010.
- [4] Y. Z. Hu *et al.*, "12.2 3D gesture-sensing system for interactive displays based on extended-range capacitive sensing," in *Proc. IEEE Int. Solid-State Circuits Conf.*, San Francisco, CA, USA, Feb. 2014, pp. 212–213.
- [5] *Microchip: MGC3130 Datasheet*. Accessed on Sep. 1, 2016. [Online]. Available: www.microchip.com/wwwproducts/devices.aspx?product=mgc3130
- [6] L. Du *et al.*, "6.7 A 2.3mW 11cm-range bootstrapped and correlated-double-sampling (BCDS) 3D touch sensor for mobile devices," in *Proc. IEEE Int. Solid-State Circuits Conf.*, San Francisco, CA, USA, Feb. 2015, pp. 122–123.
- [7] L. Du *et al.*, "Invited—Airtouch: A novel single layer 3D touch sensing system for human/mobile devices interactions," in *Proc. ACM/IEEE Design Autom. Conf.*, Austin, TX, USA, Jun. 2016, pp. 1–6.
- [8] P. Maddan and P. Kaur, *An Introduction to Capacitive Sensing*, EE times, San Jose, CA, USA, Apr. 2012.
- [9] G. Barrett and R. Omote, "Projected-capacitive touch technology," *Inf. Display*, vol. 26, no. 3, pp. 16–21, 2010.
- [10] T. Davis, *Reducing Capacitive Touchscreen Cost in Mobile Phones*, Cypress Semicond., San Jose, CA, USA, Oct. 2013.
- [11] S. N. Makarov and G. M. Noetscher, *Low-Frequency Electromagnetic Modeling for Electrical and Biological Systems Using MATLAB*. Hoboken, NJ, USA: Wiley, 2015.
- [12] ITO Sheet Resistance Standards, VLSI Standards Inc., Milpitas, CA, USA, 2012. [Online]. Available: <https://vlsistandards.com/products/electrical/ito.asp?sid=86>

- [13] mTouch Projected Capacitive Touch Screen Sensing Theory of Operation, Microchip, Chandler, AZ, USA, 2010.
- [14] L. Du *et al.*, "A 2.3-mW 11-cm range bootstrapped and correlated-double-sampling three-dimensional touch sensing circuit for mobile devices," *IEEE Trans. Circuits Syst. II, Exp. Briefs*, vol. 64, no. 1, pp. 96–100, Jan. 2017.
- [15] G. T. Carlson and B. L. Illman, "The circular disk parallel plate capacitor," *Amer. J. Phys.*, vol. 62, no. 12, pp. 1099–1105, 1994.
- [16] *HTC Salsa Phone Introduction*. Accessed on Sep. 1, 2016. [Online]. Available: https://en.wikipedia.org/wiki/HTC_Salsa
- [17] *Airtouch Demo: Single Touch*. Accessed on Sep. 1, 2016. [Online]. Available: <https://youtu.be/3ivwCi3E8Ig>
- [18] *Airtouch Demo: Multi-Touch*. Accessed on Sep. 1, 2016. [Online]. Available: https://youtu.be/OOb_1cYKtyQ
- [19] S. Xia, K. Makinwa, and S. Nihtianov, "A capacitance-to-digital converter for displacement sensing with 17b resolution and 20 μ s conversion time," in *Proc. IEEE Int. Solid-State Circuits Conf.*, Kobe, Japan, Feb. 2012, pp. 198–199.
- [20] *Samsung Smart TV Introductions*. Accessed on Sep. 1, 2016. [Online]. Available: <http://www.samsung.com/us/experience/smart-tv/>



Li Du (S'15–M'16) received the B.S. degree in information science and engineering from Southeast University, Nanjing, China, in 2011, the M.S. degree in electrical engineering from the University of California at Los Angeles (UCLA), Los Angeles, CA, USA, in 2013, and the Ph.D. degree from UCLA in 2016.

He was with the High-Speed Electronics Laboratory, UCLA, and was in charge of designing high-performance mixed-signal circuits for communication and touch-screen systems. He was an

intern with Broadcom Corporation FM radio team, in charge of designing a second order continuous-time delta-sigma ADC for directly sampling FM radios in 2012, for four months. From 2013 to 2016, he is with Qualcomm Inc., San Diego, CA, USA, designing mixed signal circuits for cellular communications. He is currently a Hardware Architect with Kneron Inc., San Diego.



Chun-Chen Liu (S'04–M'08–SM'16) received the B.S. degree in electrical engineering from National Cheng Kung University, Tainan, Taiwan, in 2003, and the Ph.D. degree from the University of California at Los Angeles, Los Angeles, CA, USA, in 2017.

From 2007 to 2010, he was a Technical Officer with Wireless Info Tech Ltd (acquired by VanceInfo, NYSE:VIT). He has served as the Technical Team Leader, managing and leading several research and production developments in Samsung, Seoul, Korea, Mstar, Hsinchu, Taiwan, and Qualcomm, San Diego, CA, USA. With his unique entrepreneurial and managerial expertise, he has successfully founded and co-founded several startups, including Tyflong Limit, Skyvin, and Rapidbridge (acquired by Qualcomm in 2012).

Mr. Liu was a recipient of the IBM Problem Solving Award based on the use of the EIP tool suite in 2007. Two of his papers were nominated as the Best Paper Award candidates at the IEEE/ACM International Conference on Computer-Aided Design in 2007 and the IEEE International Conference on Computer Design in 2008. He is currently the Chair & CTO of Kneron, San Diego.



Yan Zhang received the B.S.E. degree in electrical engineering from Arizona State University, Tempe, AZ, USA, in 2011, and the M.S. degree in electrical engineering from the University of California at Los Angeles (UCLA), Los Angeles, CA, USA, in 2014, where he is currently pursuing the Ph.D. degree in electrical engineering researching on high performance mixed signal circuits and SoCs for remote sensing applications.

He developed a mixed signal IC prototype for 3-D touch sensing as his master's thesis. In 2012, he was

an intern with Marvell Semiconductor, Aliso Viejo, CA, USA, on SoC validation and a design intern with the Mixed-Signal ASIC Group, Teradyne Inc., Boston, MA, USA, in 2015. He is a member of the High-Speed Electronics Laboratory, UCLA.

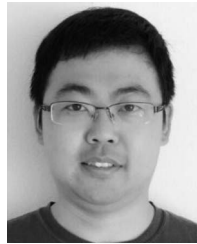


Yilei Li received the B.S. and M.S. degrees in microelectronics from Fudan University, Shanghai, China, in 2009 and 2012, respectively, and the Ph.D. degree in electrical engineering from the University of California at Los Angeles, Los Angeles, CA, USA, in 2016.

He is currently with Novumind Inc., Santa Clara, CA, USA, where he is involved in the hardware development. His current research interests include circuit and system design for emerging applications, including software-defined radio, multiband

RF interconnect, and AI acceleration hardware.

Dr. Li was a recipient of the Henry Samueli Fellowship in 2012 and the Broadcom Fellowship in 2015.



Yuan Du (S'14) received the B.S. (Hons.) degree in electrical engineering from Southeast University, Nanjing, China, in 2009, and the M.S. degree in electrical engineering from the University of California at Los Angeles, Los Angeles, CA, USA, in 2012, where he is currently pursuing the Ph.D. degree.

He is currently a Hardware Architect with Kneron Inc., San Diego, CA, USA. His current research interests include designs of machine-learning hardware accelerator, high-speed mixed-signal ICs, and

CMOS RF ICs.

Mr. Du was a recipient of the Microsoft Research Asia Young Fellowship in 2008, the Southeast University Chancellor's Award in 2009, and the Broadcom Fellowship in 2015.



Yen-Cheng Kuan (M'12) received the B.S. degree in electrical engineering from National Taiwan University, Taipei, Taiwan, and the M.S. and Ph.D. degrees in electrical engineering from the University of California at Los Angeles, Los Angeles, CA, USA.

From 2004 to 2007, he was a System Engineer with Realtek Semiconductor Corporation, Irvine, CA, USA, where he contributed to the design of ultra-wideband system-on-a-chip. From 2009 to 2016, he served as a Research Scientist with HRL Laboratories (formerly Hughes Research Laboratory), Malibu, CA, USA, where he researched on software-defined radios, compressed-sensing receivers, multirate signal processing for high-speed ADCs, and image processors.

Dr. Kuan was a recipient of the HRL New Inventor Award for his invention contribution. He is currently the MediaTek Junior Chair Professor with the International College of Semiconductor Technology, National Chiao Tung University, Hsinchu, Taiwan. He specializes in low-power architecture design and system level design for various DSP applications. He has over 20 U.S./international granted/applied patents.



Mau-Chung Frank Chang (M'79–SM'94–F'96) received the B.S. degree from National Taiwan University, Taipei, Taiwan, in 1972, the M.S. degree from National Tsing Hua University, Hsinchu, Taiwan, in 1974, and the Ph.D. degree from National Chiao Tung University (NCTU), Hsinchu, in 1979.

He is currently the President of NCTU. He was an Assistant Director with the High Speed Electronics Laboratory, Rockwell International Science Center, Thousand Oaks, CA, USA, from 1983 to 1997. He is also the Wintek Distinguished Professor of Electrical

Engineering with the University of California at Los Angeles, Los Angeles, CA, USA, where he also served as the Chair of the EE Department from 2010 to 2015. In this tenure, he developed and transferred the heterojunction bipolar transistor (HBT) integrated circuit technologies from the research laboratory to the production line (later became Skyworks). The HBT productions have grown into multibillion dollar businesses and dominated the cell phone power amplifier and front-end module markets for the past 20 years (currently exceeding 10 billion-units/year and 50 billion units in the last decade). His current research interests include high-speed electronics, integrated circuit/system designs for radio, radar, and imagers, and multiband interconnects for intra- and inter-chip communications.

Dr. Chang was a recipient of the David Sarnoff Award in 2006. He is recognized by his memberships with the U.S. National Academy of Engineering in 2008 and the Academia Sinica of Taiwan in 2012.